



**LUND UNIVERSITY**  
Faculty of Science

Master of Science thesis:

# Collimation technique for HPGe-detector gamma spectrometry in intense radiation fields

Mattias Jönsson  
Spring 2010

**Supervisors:**

Christer Samuelsson and Karl Östlund

Department of Medical Radiation Physics  
Clinical Sciences, Lund  
Lund University



## Abstract

The aim of this master thesis was to develop a rotation-based collimation system for large coaxial high-purity germanium detectors for use in intense radiation fields. A collimator was constructed formed as a cylinder surrounding the detector, with a 90° slit opening to the detector. The rotational asymmetry caused by the slit was used to trace the direction of the incident gamma rays as well as reducing dead time problems at high-count rates.

High-purity germanium detectors have an energy resolution superior to scintillation detectors such as sodium iodide and are therefore more suited for radionuclide identification. Germanium detectors are an important complement to the more effective sodium iodide detectors, which often are used in mobile in situ gamma spectrometry.

A problem with large high purity germanium detectors is often that the dead time rises and becomes too high for accurate measurements even at as low gamma dose rates as a few microsieverts per hour. Without any modifications of the detector geometry measurements could be impossible in many situations, for instance after a reactor failure scenario with release of radioactive material.

A mobile system with the collimator and detector mounted in an aluminum rack was built. The system has been tested for localization of radioactive sources. The collimator attenuates at most  $89 \pm 1$  percent of the photons at 1332 keV, which reduces the dead time significantly. By rotating the collimator the reduction of photon fluence rate could be varied from  $3 \pm 3$  percent to  $89 \pm 1$  percent.

## **Acknowledgement**

I would like to thank my supervisors Christer Samuelsson and Karl Östlund. Karl has been a great support and source of motivation and inspiration during the whole project and contributed with a lot of valuable ideas and constructive criticism.

The Swedish Radiation Safety Authority financed the project, I thank them and especially Robert Finck for all support and confidence in my work. I gratefully thank to friend and colleague Jonas Nilsson for his help with data analysis and programming. I would like to thank Lars Andersson-Ljus and Jan Hultqvist from the mechanical workshop at the oncology section at Lund university hospital who casted the collimator. The Monte Carlo code MCNP5 from the Los Alamos National Laboratory was used for the computer simulations.

Finally I would like to thank my fellow coworkers Peder Kock, André Ahlgren and Gustav Brolin for all their help and many good discussions.

# Contents

<b>1</b>	<b>Background</b>	<b>1</b>
<b>2</b>	<b>Aim</b>	<b>1</b>
<b>3</b>	<b>Previous work</b>	<b>1</b>
<b>4</b>	<b>Theory</b>	<b>2</b>
4.1	Energy resolution . . . . .	2
4.2	Spectrometry statistics . . . . .	2
4.3	Pulse processing . . . . .	2
<b>5</b>	<b>Material and Method</b>	<b>6</b>
5.1	Detector . . . . .	6
5.1.1	Definition of geometry and coordinate system . . . . .	6
5.2	Design . . . . .	7
5.2.1	Response symmetry . . . . .	7
5.3	Monte Carlo simulations . . . . .	8
5.3.1	Detector efficiency . . . . .	8
5.4	Spectrum analysis . . . . .	9
5.4.1	Background correction . . . . .	9
5.4.2	Dead time correction . . . . .	10
5.5	Collimator software . . . . .	10
5.6	Collimator characterization . . . . .	11
5.6.1	Attenuation factor . . . . .	11
5.6.2	Peak-to-Compton ratio . . . . .	11
<b>6</b>	<b>Results</b>	<b>12</b>
6.1	Collimator design . . . . .	12
6.2	Dead time correction model evaluation . . . . .	13
6.3	Detector response as function of position along $z$ -axis . . . . .	14
6.4	Angular detector response . . . . .	14
6.5	Evaluation of Monte Carlo simulation . . . . .	15
6.6	Attenuation factor . . . . .	16
6.7	Peak-to-Compton ratio . . . . .	17
<b>7</b>	<b>Examples</b>	<b>18</b>
7.1	Single source . . . . .	18
7.2	Multiple sources . . . . .	18
<b>8</b>	<b>Discussion</b>	<b>19</b>
8.1	Collimator . . . . .	19
8.2	Monte Carlo . . . . .	21
8.3	Angular asymmetry . . . . .	21
<b>9</b>	<b>Conclusions</b>	<b>21</b>

# 1 Background

Germanium semiconductor detectors have a superior energy resolution making them suitable for environmental studies. However, slow pulse processing becomes a problem in intense radiation fields. The solution to the dead time problems could be to shield the detector with an attenuating high-Z material.

An attenuator that is not isotropically shielding the detector reduces the photon fluence rate\* in the crystal and causes an asymmetric detector response, which can be utilized to give the operator information about direction of incident gamma rays i.e. locating a radioactive source or surface deposition of fallout activity.

It is an advantage to be able to use the same large HPGe-detector in extreme conditions as used for routine measurements in situ in non-elevated radiation levels by the emergency preparedness laboratories. Large HPGe-detectors have a low detection limit, and are therefore suitable for most in situ gamma spectrometry applications. Smaller crystals do not suffer from the same dead-time problem but are less suitable for radionuclide identification since the probability of full absorption of a photon is smaller.

## 2 Aim

The aim of this master thesis was to develop a method for in situ high-resolution gamma spectrometry in intense radiation fields using a collimator for non-isotropic shielding of a large coaxial HPGe-detector.

The collimator system should:

- ◇ enable measurements in intense gamma radiation fields (ambient dose rate of about  $10 \mu\text{Sv h}^{-1}$  or higher)
- ◇ be used for localization of radiation sources
- ◇ not be heavier than it can be transported by a car and carried by two persons

## 3 Previous work

The principle for collimator design with a non-isotropic shielding of the detector has previously been used with NaI-detectors e.g. by Fujiomoto [1] and with an ionization chamber by Gould et al. [2]. The 3x3 inch NaI-detector used by Fujimoto and the gas filled detector used by Gould could be operated in more intense radiation fields than large unshielded HPGe-detectors. The collimator designed by Fujiomoto was intended to get the operator the directional information by rotating the collimator around the detector. To be used in intense radiation fields the HPGe-detector must be shielded by an attenuating material.

A hand-held detector for gamma radiation monitoring constructed as a compact gamma camera with several photomultiplier tubes connected to one scintillator crystal was described by Guru et al. [3], the system produces a picture of the gamma fluence. A system that uses several separate detectors to get a directional information based on the relative response from the different detectors has been constructed for e.g. by Uher et al. [4]. The use of only one detector has the advantage of not being as sensitive to energy calibration drift and the system would therefore be more stable.

The mass of the system has been a limiting factor for reducing high-energy photon fluence rate. A heavy system must be mounted in a vehicle to be operated in the field. The Russian ministry for atomic energy (МИНАТОМ) participated in the international exercise Barents Rescue LIVEX 2001 held in Boden, Sweden [5]. A NaI-detector with a lead collimator mounted on the roof of a car was used. The collimator was in the shape of a horseshoe and surrounded the

---

\*The number of photons incident on an area during a given time. Fluence rate has the dimension  $\text{m}^{-2}\text{s}^{-1}$

detector. This collimator was placed upon a lead plate and rotated around the detector with an electric motor. No scientific publications were found that described this system in detail.

## 4 Theory

### 4.1 Energy resolution

Germanium is a semiconducting material with a small band gap. The average energy required to create an electron hole pair is 2.96 eV at 77 K [6]. Free charges, created in the crystal by photon interactions, are collected to form the pulse that will later be processed and analyzed. In scintillation systems the photon interactions causes scintillation. The energy required to get one scintillation photon in a NaI-crystal is typically 26 eV [6].

The scintillation photons in a scintillation detector and the free charges in a semiconductor detector are “information carriers”. Fluctuation in the number of information carriers produced can be described by a Poisson distribution. The mean number of information carriers will determine the uncertainty in pulse height and thus the energy resolution. Since the mean number of information carriers created by a fully absorbed photon is larger in the HPGe-crystal than in the NaI-crystal the energy resolution will be better in the HPGe-detector.

Figure 1 shows three spectrums, one from a 4 liter NaI-detector, one from a 3x3 inch NaI-detector and one from the 123% p-type HPGe-detector<sup>†</sup> used in this work, all measured at the same distance from a point like <sup>137</sup>Cs-source (185 kBq). NaI-detectors can be made in large volumes to get a good intrinsic efficiency but suffers from a poor energy resolution compared with the HPGe-detector. In this case only one isotope was of interest but the scintillation detectors still fail to fully resolve the <sup>137</sup>Cs-peak at 662 keV<sup>‡</sup> from the gamma energy at 609 keV that comes from the decay of radon progeny <sup>214</sup>Bi. Radioactive fallout and radioactive deposits after a nuclear accident or nuclear weapon detonation will consist of various radionuclides [7]. If more than one gamma energy is of interest it is easy to see the advantages in using the HPGe-detector.

### 4.2 Spectrometry statistics

With an ideal detection system the counting statistics would only depend on the statistical fluctuations of the number of incident photons and the intrinsic efficiency of the detector. Photon interaction events in the detector crystal would be randomly distributed in time and can be described by a Poisson probability density function [6, 8].

The probability of observing a photon during a time interval is constant and approximately proportional to the mean photon fluence rate in the detector i.e. the variance,  $\sigma^2$ , of a distribution describes the precision. With Poisson statistics the predicted variance is described by the equation:

$$\sigma^2 = \rho t = \mu \tag{1}$$

where  $\sigma$  is the standard deviation,  $\rho$  is probability for detecting a photon per time unit,  $t$  is the measurement time and  $\mu$  is the experimental mean. In the ideal detection system  $\rho$  is proportional to the photon fluence rate. Standard deviation can be interpreted as the uncertainty in a measurement. In gamma spectrometry the experimental mean is the number of counts and the standard deviation is the square root of the number of counts in one channel or in a peak. The variance affects the uncertainty in peak height and not the energy resolution in the spectrum.

### 4.3 Pulse processing

Dead time is the time needed for processing a pulse. The detector is unable to register any new pulses during the dead time interval. Dead time is basically a property of the analogue-to-digital

<sup>†</sup>Relative to the efficiency of a 3x3 inch NaI-detector at 1332 keV

<sup>‡</sup>The gamma photon derives from the decay of <sup>137m</sup>Ba

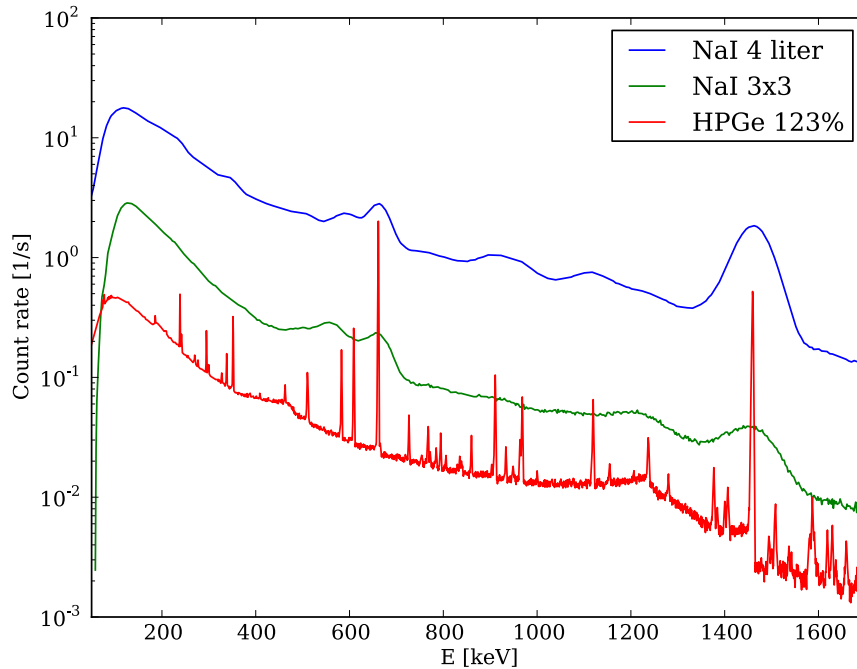


**Figure 1: Spectra from three common detector systems. The green spectrum comes from a 4 liter NaI-detector, the blue spectrum from a 3x3 inch NaI-detector and the green from the 123% p-type HPGGe-detector used in this work.**

converter (ADC) connected to the multi channel analyzer that analyzes and processes pulses. The two components will continuously be referred to simply as the multi channel analyzer. The ability to process pulses is dependent on the pulse shape and the maximum sampling frequency. Pulse shape is determined by the size of the crystal, the preamplifier and pulse shaping circuits.

The maximum count rate a detector system can be operated at is depending on pulse pile-up and dead time. Pile-up is the effect of two, or more, pulses arriving too close in time and will be interpreted as one by the multi channel analyzer. HPGGe-detectors with large crystals produce long pulses (in time), since the charge collection time is long. Scintillation detectors produce shorter pulses due to the fundamental properties of the detector type. Pile-up is less probable if the pulses are short. Analogue amplifiers have two discrimination systems for pulse rejection, one fast that sorts out true pulses from the noise background and one slower, which has the function of protecting the multi channel analyzer from pile-up.

Dead time and time lost due to pile-up rejection is basically depending of two time intervals  $T_L$  and  $T_{INS}$  [8].  $T_L$  is the time interval that is required for the multi channel analyzer to analyze one pulse. The pulse amplitude must be above a threshold voltage during  $T_L$ , see figure 4.3.  $T_{INS}$  is a time interval between two pulses needed to prevent pile-up effects. When the fast discriminator recognizes a pulse a logic pulse is sent to the multi channel analyzer opening a gate. The fast discriminator also triggers a signal during a time period called the inspection time. The inspection time is set to the expected pulse length (in time). If the fast discriminator recognizes a new pulse during the time interval  $T_{INS}$ , a gating signal will be sent to the multi channel analyzer. The gating signal inhibits the storing of the first pulse to the memory. A new pulse can not be recorded unless the remaining voltage amplitude from the previous pulse

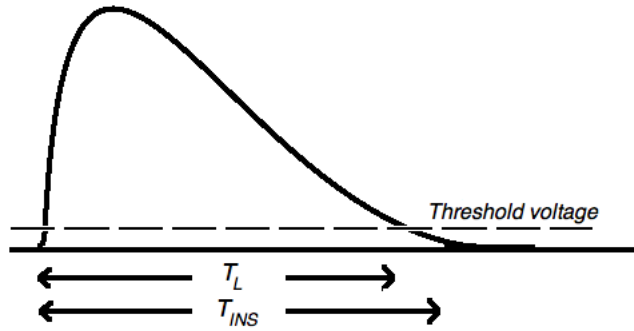


Figure 2: Illustration of threshold voltage and inspection time for pile-up protection.

is lower than a threshold voltage, even if the previous pulse was rejected. Every new pulse within the time interval  $T_{INS}$  will elongate the inhibit signal by  $T_{INS}$ . Too high pulse rates cause paralyzation of the system and all pulses will be rejected. If the inspection time is too long the previous pulse might not affect the maximum amplitude of a pulse even if the amplitude of trailing edge has not dropped below the threshold voltage before the new pulse comes although this results in the rejection of both pulses.

The term “dead time” is often used to describe the percentage measurement time lost due both to pile-up rejection and accumulated dead time in the multi channel analyzer during a measurement. A known relation between count rate and true photon fluence rate in the detector is essential for any quantitative measurements. The probability of observing a time interval between two photons arriving at the detector, providing that the photon fluence rate is constant, can be described by an interval probability density function [8]. Data could theoretically be corrected for dead time and pulse rejection losses if the time when the detector has not been active could be measured. All counting systems require a finite acquisition time to measure and record the time lost due to system paralyzation and this will induce a systematic error of information loss. System paralyzation will always affect the uncertainty of a measurement since it will always be an uncertainty in the observed dead time.

Pile-up rejection and dead time correction is the limiting factors for gamma spectrometry in intense radiation fields. Pile-up rejection will fail more often at high count rates and the uncertainty in the measured dead time will be too high for accurate spectrometry. If a primary photon and any other photon are interpreted as one, one count will be lost from the full-energy peak i.e. the primary photon fluence rate will be underestimated.

At high count rates new peaks will appear in the spectrum by superposition of primary photon pulses. The spectrums in Figure 3 demonstrate this pile-up effect. The same detectors were used as for the spectrums in Figure 1, but with a higher activity of  $^{137}\text{Cs}$ . A summation peak can be seen in the spectrum from the HPGe-detector and the large NaI-detector at 1324 keV i.e., twice the energy 662 keV from  $^{137}\text{Cs}$ . The pile-up peak is almost undetectable in the spectrum from the 3x3 inch NaI-detector.

The count rate is not proportional to the photon fluence rate at high count rates due to the pile-up effect and uncertainty in dead time correction. Gamma spectrometers should not be used at high count rates for quantitative measurements since the uncertainty will be too large [6, 8, 9].

Dead time and pile-up problems can be reduced by adjusting pulse filtering parameters in the amplifier. The amplifier used in this work shapes the pulse into a quasi-trapezoid [10]. Filtering the pulse makes it more suitable for processing by the multi channel analyzer [9], which speeds up the process. More complexly shaped pulses will decrease the uncertainty in the measured pulse height but will elongate the inspection time needed. The quasi-trapezoidal shape is described by four parameters. Rise time and Cusp control how the pulse amplitude

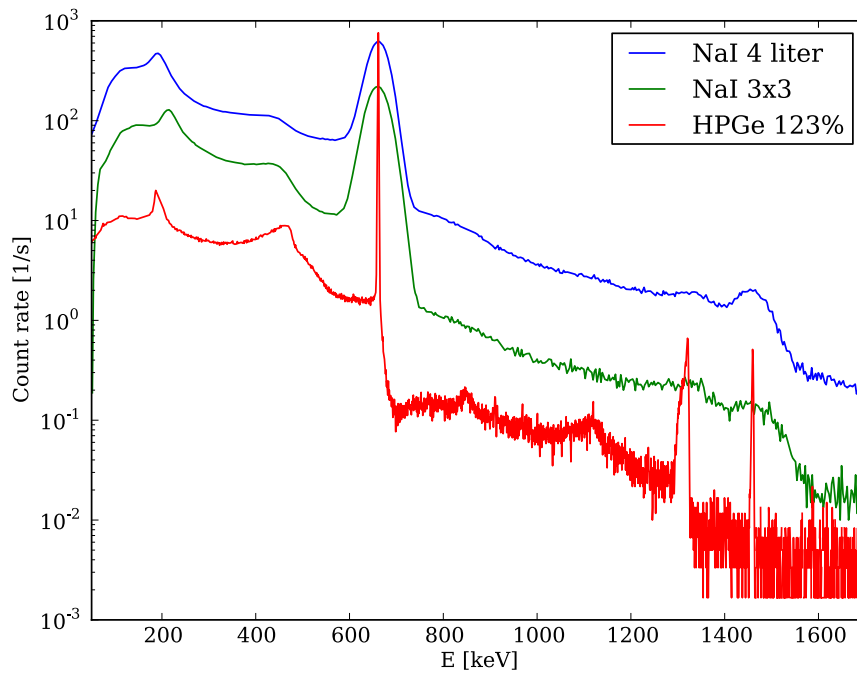


**Figure 3: Spectrum from three common detector systems. The green spectrum comes from a 4 liter NaI-detector, the blue spectrum from a 3x3 inch NaI-detector and the green from the 123% p-type HPGe-detector used in this work.**



**Figure 4: The HPGe-detector connected to DigiDART.**

risers and falls. Rise time is defined as the time for a pulse to rise from 10% to 90% of its maximum amplitude [6, 9]. Changing the rise time has the effect of spreading or narrowing the quasi-trapezoid symmetrically. Cusp controls the curvature of the sides of the trapezoid. The parameters Flattop and Tilt control the width and shape of the plateau.

If the shaping time of the amplifier circuit is comparable to the pulse rise time, fluctuations in pulse rise times will affect the final pulse amplitude. The difference in the pulse height is referred to as the ballistic deficit [9]. As the charge collection time is longer for larger crystals, the effect will be more pronounced. Reducing the rise time of the shaping circuit will decrease the pile-up problem but also reduce the energy resolution, since the uncertainty in pulse height becomes larger [10].

## 5 Material and Method

### 5.1 Detector

The detector, shown in Figure 4, used in this project was an ORTEC p-type ruggedized coaxial High-Purity Germanium detector with the relative efficiency of 123%<sup>§</sup> (ORTEC GEM 100-S serial no. 46-P41629A). The detector was connected to a portable MCA unit, (ORTEC DigiDART serial no. 06079478). The DigiDART houses all electronics needed such as multi channel analyzer, amplifier, high voltage supply and battery. The DigiDART was connected to a laptop with an USB-cable, but can also be operated as a standalone unit without the computer.

#### 5.1.1 Definition of geometry and coordinate system

A Cartesian coordinate system, shown in Figure 5, was used to describe geometries both in experiments and in the Monte Carlo simulations. Origin was set to the centre of the aluminum endcap. The  $z$ -axis was defined as the vector parallel to the central electrode. The  $x$  and  $y$ -axes defined the plane orthogonal to the central electrode. The angle  $\theta$  was defined as the angle between two vectors in a plane orthogonal to the  $z$ -axis.

<sup>§</sup>Relative to the efficiency of a 3x3 inch NaI-detector at 1332 keV

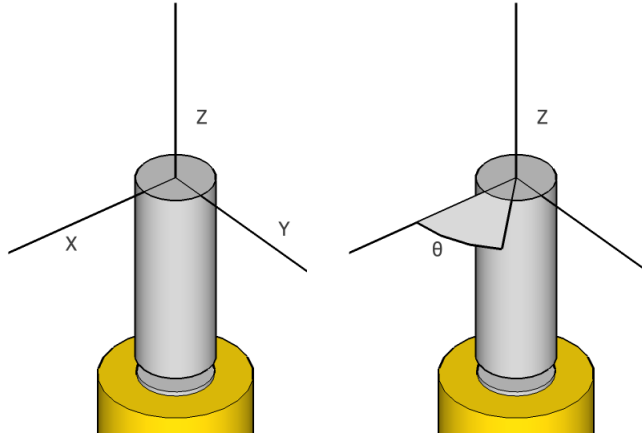


Figure 5: Definition of a Cartesian reference system.

## 5.2 Design

The design would be a further development of the basic idea of a rotating collimator surrounding the detector used e.g. by Fujimoto and the Russian team at Barents Rescue to be more suited for HPGe-detectors. A cylindrical collimator design with an open slit was chosen to reduce the photon fluence rate from all directions but one solid angle. The slit would form a  $90^\circ$  gap in the collimator side, the choice of angle will be discussed in section 8.1.

Rose's alloy was chosen as collimator material. The alloy consists of about 50 percent bismuth, 25 percent tin and 25 percent lead. The exact isotopic composition in the used material was unknown. Rose's alloy was more suited to processing than other high-Z materials such as lead or tungsten.

Mass was to be a limiting factor. Fifty kilogram was considered a reasonable upper mass limit if the system should be portable in the sense that it could be carried. A computer model of the collimator was made in the Monte Carlo code MCNP5 to investigate optimal wall thickness.

The mounting of the collimator had to be robust to support both the detector and collimator. An aluminium construction was chosen because of the stability and low massattenuation coefficient.

### 5.2.1 Response symmetry

In laboratories, HPGe-detectors are often used with the radioactive sample placed in front of the detector, angular response is therefore of minor concern. The proposed collimator design would require that the detector response was rotational symmetric. Inhomogeneous charge collection in the crystal would cause an asymmetric detector response. The detector response was investigated to find any local imperfections in the crystal.

A 70 mm thick block of Rose's alloy with a hole drilled through the block was used as a pencil beam collimator. The diameter of the hole was 1.5 mm and a  $x/y$ -table with the precision 0.01 mm was used to move the collimator block along the detector endcap surface. A point like  $^{133}\text{Ba}$ -source (240 kBq) was fixated in the centre of the collimator hole, as demonstrated in Figure 6. The isotope was chosen because of its low photon energies at 82 keV and 356 keV. Low energy photons in pencil beam geometry would mainly cause ionizations in the crystal surface.

The pencil beam was directed perpendicular to the central electrode. The distance between the collimator and the detector surface was adjusted with a feeler gauge to 4.0 mm. The detector was first scanned along the  $z$ -axis with the pencil beam to determine the active detector volume. The measurement was evaluated for the net peak area at 356 keV.

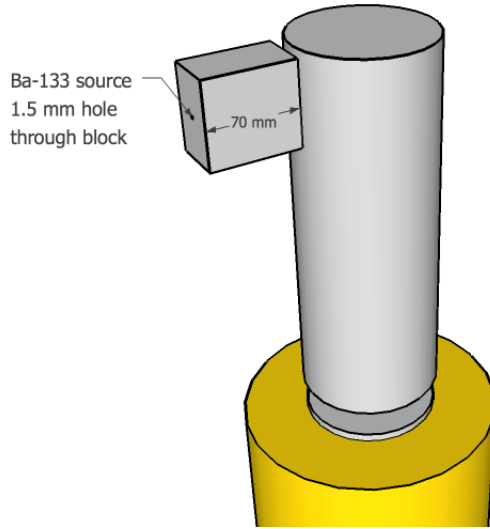


**Figure 6: Pencil beam geometry for determine rotational symmetry.**

The detector was scanned at the distances 20, 40 and 60 mm from the endcap ( $z=-20, -40, -60$ ). The detector was turned 30 degrees around the  $z$ -axis and measured at the same distances from the endcap. The measurement was repeated every thirtieth degree to cover the whole crystal surface.

### 5.3 Monte Carlo simulations

A model of the detector was constructed in the Monte Carlo simulation software MCNP5 (version 1.40). The purpose of the computer simulations was to determine a suitable wall thickness and optimum shape of the slit.

The Monte Carlo model of the detector was based upon the specification from the manufacturer. The cross section library for photon interaction MCPLIB02 was used. The library contains stopping-power values and cross sections for incoherent, coherent and photoelectric interaction and pair production [11]. Since no information about density or the isotopic composition of the crystal and the lithium and bromide contact surfaces could be obtained from ORTEC, the natural occurring isotopic composition of germanium determined by Changa et al. [12] was used in the Monte Carlo simulations.

The output from the simulations was a pulse height spectrum, which is a distribution of probabilities that a specific amount of energy would be deposited in the crystal per simulated photon i.e., equivalent to a spectrum with the probability of registering one count. The GEB input card (Gaussian energy broadening) in MCNP5 was used to simulate peak height uncertainty. Coefficients for the GEB card were calculated, as instructed in the MCNP5-manual, by measuring the FWHM-value at different energies in spectrums measured at different count rates.

#### 5.3.1 Detector efficiency

Crystal density in the computer model was chosen by simulating different crystal densities and compare results with experimental data, the choice will be discussed in section 8.2. The density of the crystal was first estimated by measuring the density of a smaller germanium crystal from a broken n-type HPGe-detector. The density was measured by weighing the crystal and than lowering it into a beaker filled with water to measure the volume. The surface tension was not considered in the uncertainty calculation. Since the crystal of the old detector was not identical

to the crystal in the simulated detector the crystal density were only used as the parameter to get a better correlation between measured and simulated data.

To evaluate the computer model and find the right crystal density a geometry similar to the collimator case was used. Since the crystal would be partially irradiated through a slit the probability of detecting a photon would not only be dependent of the density of the crystal, but also of the slit shape.

Two lead bricks were placed in front of the detector to form a slit as demonstrated in Figure 7. The detector is seen to the right in the picture. A point like radioactive source was placed 25 cm from the detector surface to irradiate the detector through the slit. The radionuclides  $^{137}\text{Cs}$  (185 kBq) and  $^{60}\text{Co}$  (161 kBq) were used as photon sources i.e. the efficiency evaluation were made with the photon energies 662, 1173 and 1332 keV.

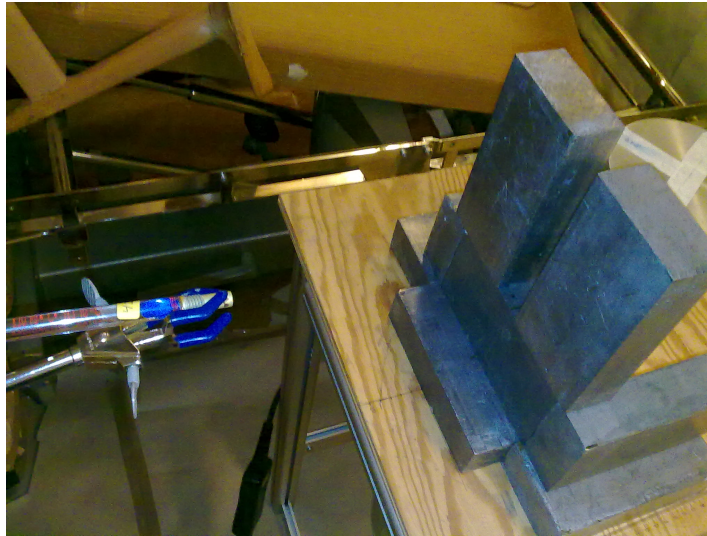


**Figure 7: Experimental setup for evaluation of simulated detector efficiency.**

Low activity sources were chosen to get minimal dead time effects in the spectrum. The measurements were conducted in a low activity laboratory at Lund university hospital to get as low background contribution as possible. The distance between the two lead bricks was varied to change the photon fluence rate in the crystal but also to change the irradiated crystal volume in the same manner as the collimator would do.

The same geometry was built in the Monte Carlo simulation program MCNP5. Four crystal densities from  $4.9 \text{ g cm}^{-3}$  to  $5.2 \text{ g cm}^{-3}$  were simulated. The density was set to the same value for the whole crystal and the same isotopic composition was used in both the lithium-drifted layer and the boron contact layer on the crystal surface. The experiment was evaluated by comparing simulated data to experimental data to determine which crystal density to use in all future simulations.

## 5.4 Spectrum analysis

A simple computer program was written for extracting data from spectrum files and analyzing the data. The program was developed to the final software for the collimator system.

### 5.4.1 Background correction

For extraction and background correction of the peak area obtained from the spectrum, a version of the triple-window method was used. In the spectrum successive channels represent increasing energy deposited in the detector crystal and a gamma ray, fully absorbed in the crystal, will

appear as a distribution of counts in the spectrum. The distribution is approximately Gaussian about a central channel [6, 9]. Since the peaks are only a few kiloelectron volts wide the approximation was made that the background was linear in a region around a peak. The spectrum in a region around the peak could then be described by the following equation:

$$\text{Counts}(\kappa) = C_{\text{Gauss}} e^{-\frac{(\kappa-\mu)^2}{2\sigma^2}} + C_{\text{Linear}} \kappa + C_{\text{Constant}} \quad (2)$$

where  $\kappa$  is the channel number,  $C_{\text{Gauss}}$  is a constant,  $\sigma$  is the standard deviation of the distribution,  $\mu$  is the centroid channel in the peak and  $C_{\text{Linear}}$  and  $C_{\text{Constant}}$  are constants describing the background.

The peak area analysis was done by fitting the Gaussian function to a region of interest around each peak in the spectrum with the least square method. The background calculated using the optimized parameters,  $C_{\text{Linear}}$  and  $C_{\text{Constant}}$ , was then subtracted from the region of interest around the peak.

#### 5.4.2 Dead time correction

DigiDART uses the extended live time correction according to Gedcke-Hale method, which elongates the acquisition time during the measurement to compensate for time lost [8]. The guaranteed accuracy within  $\pm 3\%$  for the count rates up to 50 000 counts per second.

The dead time correction model was evaluated by an experiment where a point like  $^{60}\text{Co}$  (161 kBq) source were placed in front of the detector so that the dead time was about five percent. To vary the count rate a point like  $^{137}\text{Cs}$  (370 MBq) source was also placed on a trolley in front of the detector. In theory, if the pile-up rejection and dead time correction model works, the area of the cobalt peaks not change more than  $\pm 3\%$  as the cesium source is moved towards the detector to increase the dead time. The trolley with the cesium source was moved towards the detector in small steps and a spectrum was obtained at each position. The live time clock was set to 600 seconds.

### 5.5 Collimator software

Software for the collimator was written in the programming language Python (version 6.1). The first version of the software analyses spectrums obtained at different angles and calculates the direction of incident gamma rays at different energies to find radioactive sources.

The program can either be used with a peak-finding algorithm that loops through an energy spectrum or with an algorithm that only analyzes the spectrum at specific gamma energies for common radionuclides defined in a library. Only using the specific gamma energies would take less time than if the whole spectrum is searched through, but isotopes might be missed and the method would also be depending on a good energy calibration.

All spectrum files should be saved in one specific directory and named after the angle the slit was directed at. The directory location was to be the only input data required to run the collimator software.

The software was divided in two parts. The first part was a loop though all the spectrum files (\*.spe) in a selected directory to extract data from the files. The background correction model described in Section 5.4.1 was used in the peak-finding algorithm with energies evenly distributed within an energy interval as starting value for centroid energy.

Optimized parameters were compared to predefined criterions. Successive curve fits would indicate that a peak had been found in the spectrum. If the nuclide libraries were used only the predicted photon energies were examined. The number of angles where the curve fits fulfilled the criterions was used to evaluate if a radioactive source actually had been found.

Due to the high attenuation factor, low energy gamma peaks will only be visual in the spectra if the collimator slit is directed towards the source of radiation. To calculate the direction to the source, peak area must be calculated even for angles where the peaks cannot be distinguished in the spectra. A background subtraction model that works even in the case were the curve

fit fails was developed. The optimized parameters are used if the curve fit was successful and otherwise not. The method was tried out by trial-and-error to fit the source-finding algorithm.

The count rate was expected to be higher when the collimator slit was directed at a radioactive source. If the detector response was plotted as a function of angle it could be assumed that the response was symmetric around the angle at which the slit was directed towards the source. The angle was found by fitting a pyramid function (equation 3) to the peak areas as function of incident angle.

$$f(\theta) = C_1 \cdot |\theta - C_2| + C_3 \quad (3)$$

The pyramid function is a function of incident angle of the incident photon rays.  $C_1$ ,  $C_2$  and  $C_3$  are the coefficients for optimization and  $\theta$  is the incident angle. The optimization tool finds the angle  $C_2$  where the area under the curve left of  $C_2$  is equal to the area right of  $C_2$ . The pyramid fit could unfortunately not be used for finding the peaks since the optimization tool used often fails if the starting parameter for  $C_2$  was not good enough. To find good starting values for  $C_2$  the arithmetic mean of three concatenate data points was compared with the data in a larger region around the three data points, this to roughly find the local maxima. The optimized values of  $C_2$  and the number of successive fits were returned as a possible direction to a radioactive source if the number of successive curve fits were larger than a predefined threshold. Two examples will be described in section 7, where the software has been tested with both a single and multiple sources.

## 5.6 Collimator characterization

### 5.6.1 Attenuation factor

The reduction of photon fluence rate was quantified by a factor defined as the ratio of the detector responses with the collimator and without the collimator:

$$\text{Attenuation factor} = \frac{\text{Detector response without collimator}}{\text{Detector response with collimator}} \quad (4)$$

By rotating the collimator the attenuation factor can be varied from its maximum to its minimum.

A point like radioactive source was placed two meters from the detector. The isotopes  $^{133}\text{Ba}$  (28 MBq),  $^{137}\text{Cs}$  (18 MBq),  $^{60}\text{Co}$  (22 MBq) and  $^{226}\text{Ra}$  (10 MBq) were chosen to cover photon energies from 82 to 2447 keV. Three series of measurements were made for each isotope, one with the collimator slit directed at the source, one with the slit directed from the source and one without the collimator. Detector response was defined as the background corrected peak count rate.

### 5.6.2 Peak-to-Compton ratio

Peak-to-Compton describes the fraction of primary photons that are registered in the photo peak, i.e. a way to quantify the quality of a spectrum.

To measure the Peak-to-Compton a point like  $^{60}\text{Co}$ -source (22 MBq) placed two meters from the detector. Three series of measurements was made, one with the collimator slit directed at the source, one with the slit directed from the source and one without the collimator.

Peak-to-Compton was calculated according to the method described by the Institute of electrical and electronics engineers Inc. [13]. The Compton region was defined by the channel interval closest to the interval 1040 to 1096 keV.

## 6 Results

### 6.1 Collimator design

The final Monte Carlo model, seen in Figure 8, was used as the blueprint for constructing the collimator. The collimator had to be casted in four pieces due to the volume of the crucible. The slit extended over two of the rings and the junctions between the parts were constructed so that there are no chinks were the radiation could pass through.

The final mass of the prototype was 48.6 kilograms divided in four parts, three parts for the cylinder and one lid. The outer diameter of the collimator was 214 mm, the height 235 mm, the inner diameter 124 mm and the thickness of the lid was 21 mm. The height of the slit was 149 mm. The opening angle was made  $90^\circ$ . The distance between the detector endcap surface and the collimator was 5 mm in all directions.

The collimator was mounted in the aluminum rack seen in Figure 9. The rack was made adjustable to support detectors with different cryostats.

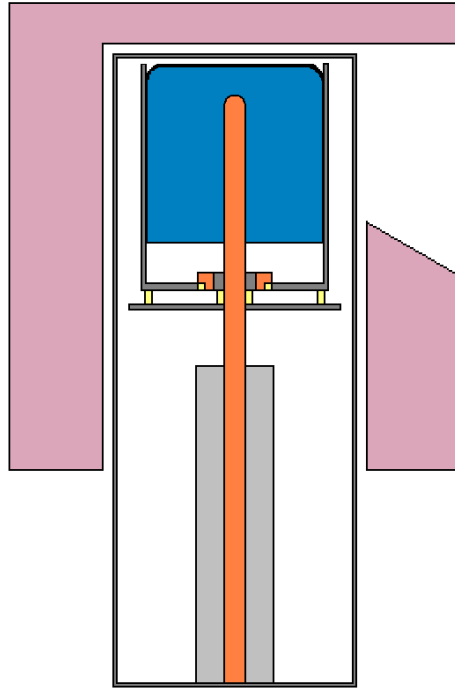


**Figure 8:** Monte Carlo model of detector and collimator. Cross-section along the  $z$ -axis. Collimator coloured in pink, germanium crystal in blue and central electrode in orange.



Figure 9: Collimator and detector mounted in the aluminium rack.

## 6.2 Dead time correction model evaluation

Experiment confirms that dead time correction model guarantee of  $\pm 3\%$  accuracy in count rates up to 50 000 counts per second was fulfilled. Result shown in Figure 10.

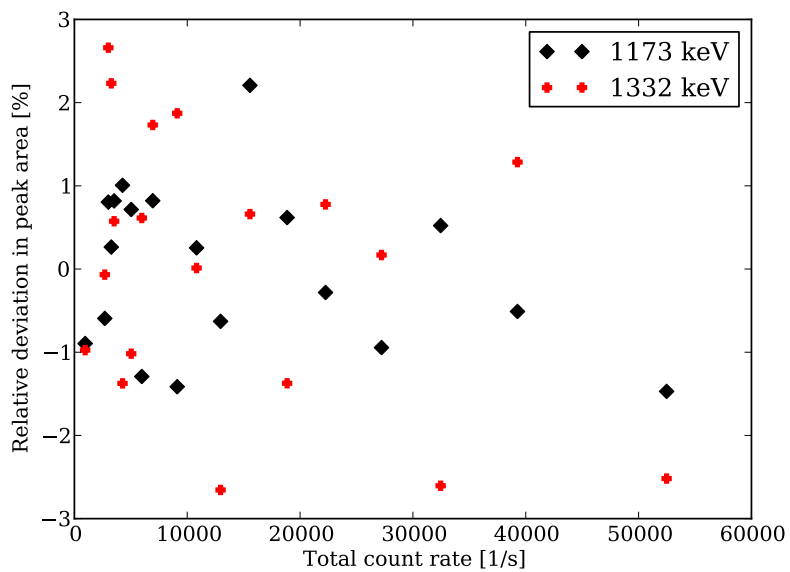


Figure 10: Experimental evaluation of the dead time correction used by the DigiDART.

### 6.3 Detector response as function of position along $z$ -axis

Experiment showed that the effective detector volume stretches from about  $z=-5$  mm to about  $z=-80$  mm as seen in Figure 11.

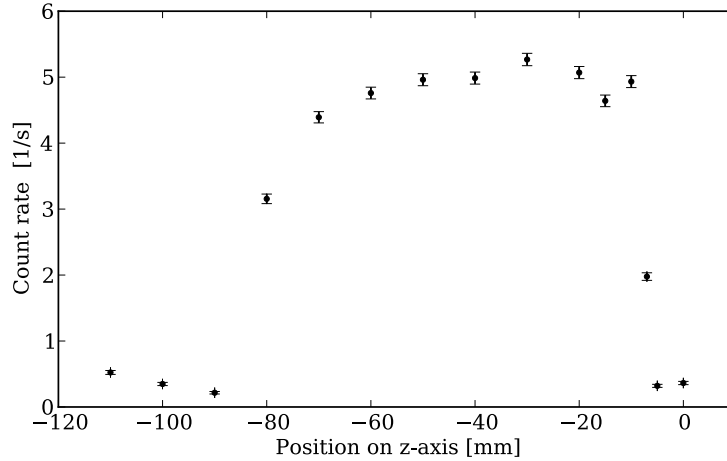


Figure 11: Detector response along  $z$ -axis. Detector response refers to net count rate in the 356 keV photo peak.

### 6.4 Angular detector response

The angular dependence was measured at  $z=-20$  mm,  $-40$  mm and  $-60$  mm. The experiment showed that the response is not entirely symmetric as seen in Figure 12 and Figure 13. The response in the 356 keV peak dropped at  $\theta = 90^\circ$ . The reference angle was chosen arbitrary.

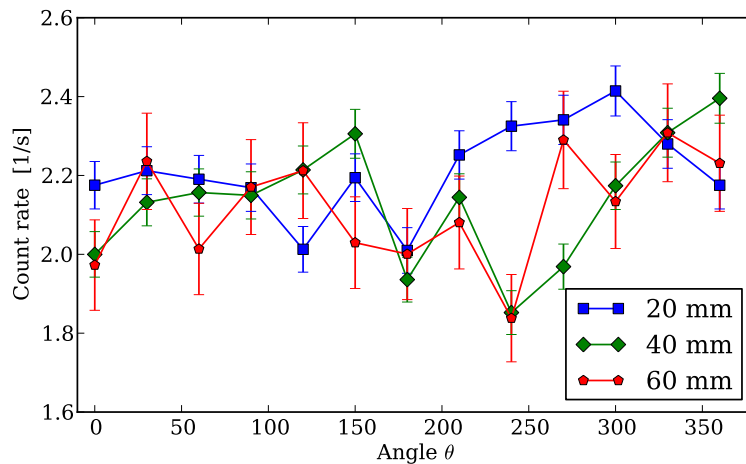


Figure 12: Angular response at 81 keV. Detector response refers to net count rate.

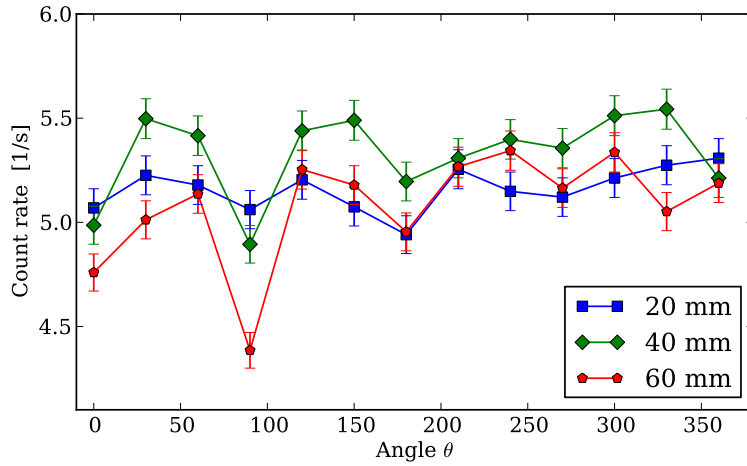


Figure 13: Angular response at 356 keV. Detector response refers to net count rate.

### 6.5 Evaluation of Monte Carlo simulation

The density of the n-type crystal was  $5.21 \pm 0.05 \text{ g cm}^{-3}$ . The results of the Monte Carlo simulation showed that the model overestimated the photon fluence at low photon energies and underestimated photon fluence at higher energies. The model predicted the photon fluence within  $\pm 6\%$  at the highest photon energy for 2 to 6 cm slit widths. The density of about  $5.1 \text{ g cm}^{-3}$  was chosen as the best value to describe both low and high photon energies. Results shown in Figures 14, 15 and 16.

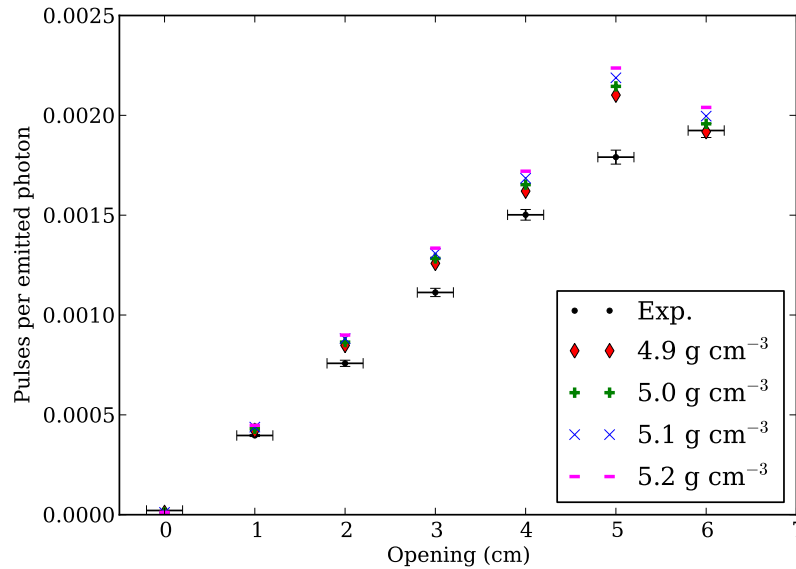
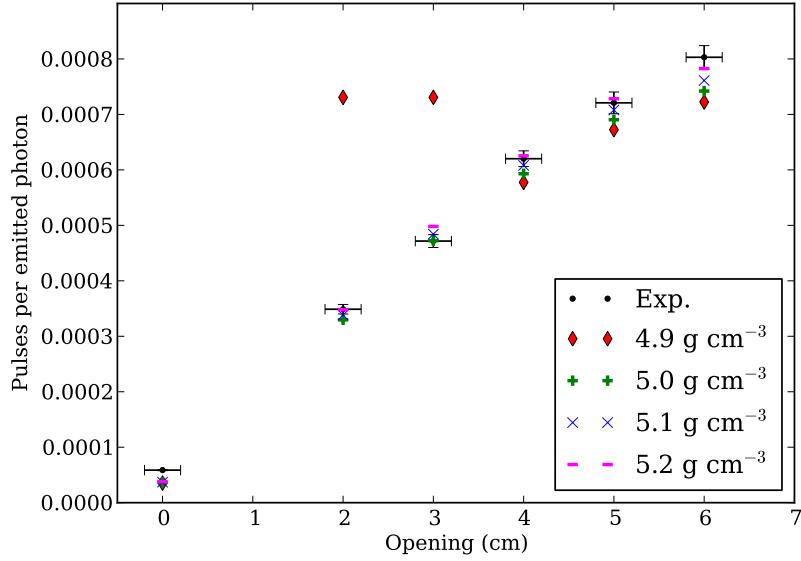
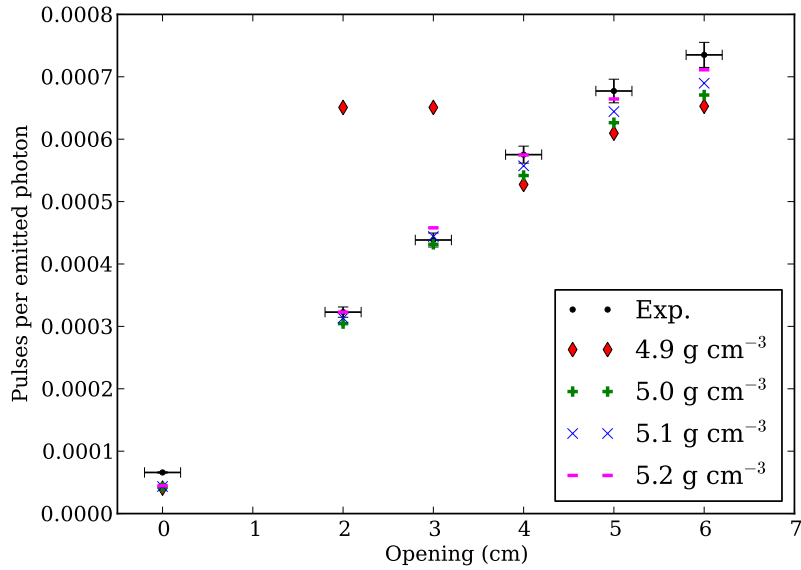


Figure 14: Simulation and experimental measurement of detector response at 662 keV.



**Figure 15: Simulation and experimental measurement of detector response at 1173 keV.**



**Figure 16: Simulation and experimental measurement of detector response at 1332 keV.**

## 6.6 Attenuation factor

Attenuation factor was defined as the ratio of detector response with and without the collimator. The maximum reduction in photon fluence rate i.e., when the collimator slit were directed from the source of radiation is presented in Figure 17. The maximum attenuation factor could not be

calculated for the barium energies 82, 303 and 356 keV since the peaks could not be distinguished from the background. At 662 keV was the attenuation factor about 100 but drops rapidly. At 2447 keV ( $^{214}\text{Bi}$ ) the measured attenuation factor was  $6.3 \pm 0.2$ . The Figure 18 shows the minimum attenuation factor i.e. when the collimator slit was directed to the radiation source. The peak area was almost unaffected by the collimator in this configuration.

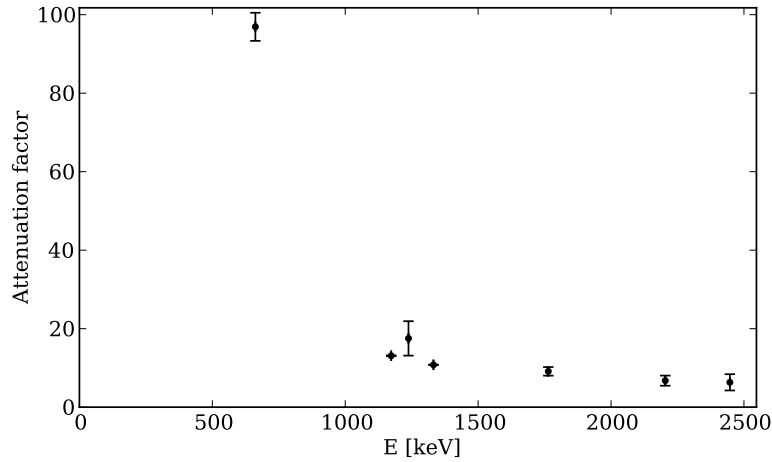


**Figure 17:** Attenuation factor with the collimator slit directed away from the source.

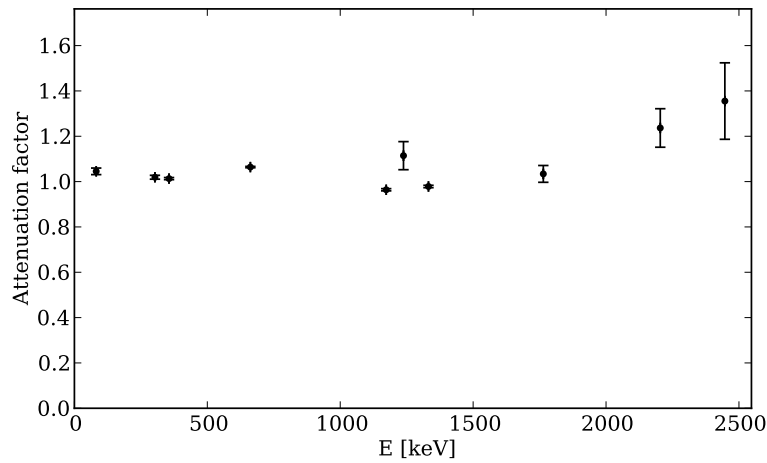


**Figure 18:** Attenuation factor with the collimator slit directed towards the source.

## 6.7 Peak-to-Compton ratio

The Peak-to-Compton ratio for  $^{60}\text{Co}$  is presented in table 1.

**Table 1: Peak-to-Compton ratio**

Without collimator	Collimator directed to source	Collimator directed from the source
$69 \pm 0.7$	$71 \pm 2$	$40 \pm 0.9$

## 7 Examples

### 7.1 Single source

A  $^{137}\text{Cs}$  source with the activity 185 kBq was placed one meter from the detector. Measurement was made in an office and not in the low-activity laboratory used for other measurements in this work. Measurements were made every ten degrees with the collimator directed at the source at zero degrees. All spectrum files was saved in one specific directory. The result of the run was that the software managed to identify a  $^{137}\text{Cs}$ -source at an angle 2 degrees from the null-angle with 13 successive Gaussian fits. The calculations took about 8 seconds when the nuclide list was used. Figure 19 shows the total count rate and count rate in the cesium full-energy peak as function of collimator direction.

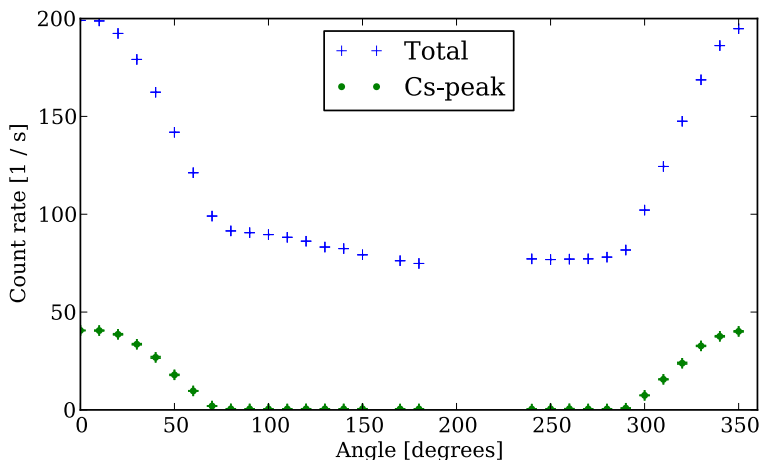


Figure 19: Peak area and total count rate as function of angle.

### 7.2 Multiple sources

Three sources were placed around the detector, one  $^{137}\text{Cs}$ -source with the activity 37 MBq, one  $^{137}\text{Cs}$ -source with the activity 40 MBq and one  $^{133}\text{Ba}$ -source with the activity 28 MBq. The directions from the collimator to the sources were approximately 25, 280 and 350 degrees and the distance about two meters. The radioactive sources were placed arbitrary and the angle was measured with a compass, the accuracy was about  $\pm 3$  degrees.

The dose-rate at the detector was  $44 \mu\text{Sv h}^{-1}$  (measured with an Exploranium GR135, calibrated to ambient dose equivalent). Measurements were made every ten degrees. The collimator software identified the following sources.

- ◇  $^{133}\text{Ba}$  (302 keV) at the angle 348 degrees with 13 successive Gaussian fits.
- ◇  $^{133}\text{Ba}$  (356 keV) at the angle 350 degrees with 13 successive Gaussian fits.
- ◇  $^{137}\text{Cs}$  (662 keV) at the angle 24 degrees with 32 successive Gaussian fits.
- ◇  $^{137}\text{Cs}$  (662 keV) at the angle 282 degrees with 32 successive Gaussian fits.

The software failed to find the 82 keV full energy peak of  $^{133}\text{Ba}$ . These results showed that the software manages to find multiple sources. Figure 20 shows the count rate in the cesium and two barium full-energy peaks as function of collimator direction and Figure 21 the total count rate as function of direction.

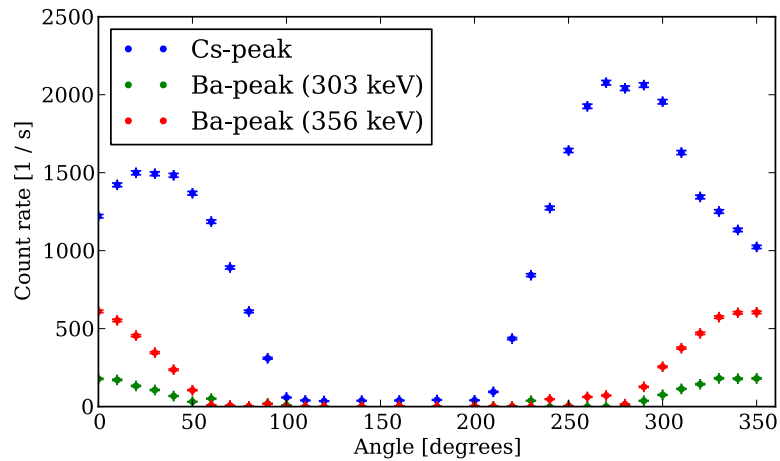


Figure 20: Peak area as function of angle.

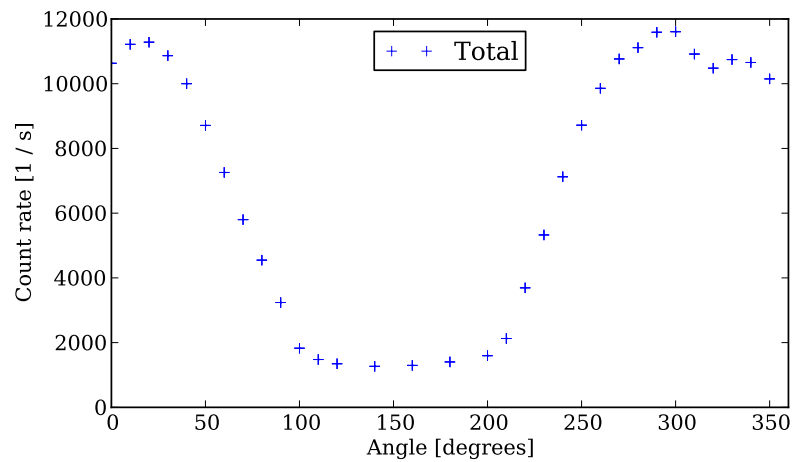


Figure 21: Total count rate as function of angle.

## 8 Discussion

### 8.1 Collimator

With the collimator, spectra at higher dose rate can be obtained. Since the intention was to use the collimator for in situ measurements, by the emergency preparedness laboratories, the wall thickness was chosen thick enough to reduce the photon fluence rate even at high photon energies. Low photon energies would not require as thick wall as was chosen, but only one collimator was constructed.

If the radiation field is monodirectional i.e. most of the radiation comes from one direction the collimator can be rotated to adjust the dead time to a level suitable for an accurate measurement without reducing the energy resolution. The attenuating material affects the spectrum and the contribution from photons scattered in the collimator cause problem at the low-energy part of the spectrum.

Peak-to-Compton ratio, in this case can be interpreted as a measure of photons scattered outside the crystal. With the collimator slit directed towards the source of radiation the ratio was not significantly lower than without the collimator. The ratio shows that the contribution of photons scattered in the collimator wall do not distort the spectrum if the slit is directed towards the source. The contribution of photons scattered in the collimator was significantly higher when the slit was directed from the source.

The design of the collimator was first made in the Monte Carlo program but was changed continuously during the construction of the prototype due to limitations with the casting and with the milling and lathing machines.

The angle of the slit was chosen large enough to not affect the photon flux from one direction of interest but narrow enough to get a robust construction. An insertable module fitting into the collimator slit was planned. The module would narrow the slit, but was not included in this thesis due to time constraints. The number of measurements at different angles needed to get directional information would be dependent on the slit opening-angle. A collimator with a wider opening angle would require less measurements to find one point-like radiation source than with a narrow slit, but would reduce the possibility to discover more than one source of radiation.

The collimator software developed for analyzing single spectrums and series of spectrum for finding the direction to possible sources of radiation has shown to be usable and has managed to find several point-like sources. Figure 20 and 21 illustrate the advantage of using a detector with an energy resolution good enough for resolving multiple gamma peaks. When only the full energy peaks were studied the angular dependence was larger than as the whole spectra was studied since scattered photons were discriminated. A curve fit algorithm in the collimator software calculates the angle. The uncertainty in the proposed angle is dependent of the statistical uncertainty of the data, the background subtraction and on how well the starting values for the optimization parameters are estimated. The uncertainty in the direction that the software propose is dependent on the number of measured angles and the number of counts in the full energy peak and could not be quantified in any general case.

For high energy photons the attenuating factor of the collimator was the limiting factor since the angular dependence becomes smaller and the source-finding algorithm does not manage to find the source of radiation. For low energy photons the limiting factors were both the background correction model and the source-finding algorithm. The collimator attenuated almost all primary photons at relatively low energies. The background correction model used was based upon an optimization of a Gaussian function with a linear background. The optimization failed when the peak was small compared to the background. The solution was to use a different background correction when the optimization failed. The source-finding algorithm also uses an optimization tool to find local maxima in the series of peak areas at different angles and the series were therefore approximated to a continuous function of angle. The solution to the problem, described in the section collimator software, was shown to be robust and motivated the use of function optimization both in the background correction of the peaks and in the source-finding algorithm. The Gaussian fit method for background correction had the advantage of not being as dependent of exact knowledge of the centroid channel as other methods for background correction such as the triple-window method and could also be used to measure energy resolution and photon energy.

## 8.2 Monte Carlo

Monte Carlo simulations made reasonable predictions of the detector response that was experimentally obtained, although the simulations seem to have failed at several times as seen in Figures 14, 15 and 16. These discrepancies were not always easy to identify and could often only be seen when a series of simulations were made where only one parameter was changed. In the Figure 14 either the simulation of the 5 cm opening or the 6 cm opening has failed. In the Figure 15 and 16 the simulation failed with the crystal density  $4.9 \text{ g cm}^{-3}$  at two opening widths. No physical explanation to the result could be thought of and troubleshooting the Monte Carlo input code gave no result. The only differences between the simulations were the density of the crystal cell or the distance between the two lead blocks, which formed the slit.

Due to the unreliable results Monte Carlo was only seen as a tool that gave a rough estimation of reality. The computer models were never adjusted to fit finished collimator. Results from the simulations of the Rose's alloy collimator are not presented in this report since the data were not compared with any experimental data due to lack of time.

Crystal density was chosen as an optimization parameter to adjust the intrinsic efficiency of the simulated detector. The density of the true crystal could be accurately measured, and other parameters optimized, but this simple approximation was found to give acceptable results.

## 8.3 Angular asymmetry

An intrinsic angular asymmetry, due to inhomogeneities in the crystal, may exist. Experiment showed that the response in the 356 keV peak dropped at one angle in the lower part of the crystal. No drop in response was seen in the 82 keV peak indicating that the inhomogeneity was probably not located in the surface of the crystal. Control of the pencil beam direction was the major source of uncertainty in this experiment. Uncertainty in the measurements was shown to be highly dependent of the experimental setup and the error was therefore estimated by redoing the measurements in one angle. The results differed with as much as five percent between two measurements at the same angle after rotating detector 360 degrees. Because of the large uncertainty in experimental set-up and poor statistics this experiment could not show any intrinsic angular dependence in the detector crystal.

The pyramid fits seemed to be wider at low photon energies than the pyramid fits for higher energy photons. The opposite behavior was expected due to the penumbra effect. The Monte Carlo simulations did not show any such difference between high and low energy photons. This effect might be explained by the higher cross-section for elastic scattering for the lower energy photons. Photons could be scattered in the air gap or aluminum between the collimator inner surface and the crystal. The source-finding algorithm only analyzes the full-energy peak to discriminate photons that has undergone any scattering outside the detector. Elastic scattering do not reduce the photon energy as much as inelastic scattering i.e. photons might still be registered in the full-energy peak after elastic scattering. The effect does not affect the accuracy of the peak finding algorithm but it will make the minimum angle between two detectable sources wider for low energy gamma photons.

## 9 Conclusions

High-resolution gamma spectrometry suffers from problem with too high dead time in intense radiation fields. An attenuating material will be necessary if a large HPGe-detector shall be used in high dose rates without a reduction of the pulse processing time.

Our work concludes that a rotating collimator with a slit could lower the dead time several times even for photon fields with high energies but still be light enough to be carried and transported. Collimation that causes an asymmetric detector response can be used for monitoring radiation fields and determine the direction of incident gamma rays.

## References

- [1] K. Fujimoto, “A simple gamma ray direction finder,” *Health Physics*, vol. 91, pp. 29–35, 2006.
- [2] E. S. K. Robert Gould, James E. Tarpinian, “An automated system for gamma radiation field mapping,” *Nuclear Instruments and Methods in Physics Research*, vol. 299 (1-3), pp. 538 – 543, 1990.
- [3] K. G. Guru S.V., He Z.; Wehe D.K., “A portable gamma camera for radiation monitoring,” *Nuclear Science Symposium and Medical Imaging Conference, 1994., 1994 IEEE Conference Record*, vol. 1, pp. 367–370, 1995.
- [4] J. J. P. S. T. G. V. Z. Uher J., Frojdh C., “Directional radiation detector,” *2007 IEEE Nuclear Science Symposium Conference Record*, vol. 2, pp. 1162–1165, 2007.
- [5] B. L. Tomas Ulvssand, Robert R. Finck, “Nks/srv seminar on barents rescue 2001 livex gamma search cell,” pp. 237 – 239, 2002.
- [6] G. F. Knoll, *Radiation Detection and Measurement, third editon*. Wiley, 2000.
- [7] *UNSCEAR 1988 REPORT Annex G Exposures from the Chernobyl accident*. 1988.
- [8] G. R. G. D. Jenkins, R., *Quantitative X-ray Spectrometry*. Marcel Dekker, New York, 1981.
- [9] G. Gilmore, *Practical Gamma-ray Spectrometry, second edition*. Wiley, 2008.
- [10] ORTEC, *Maestro-32 Software User’s Manual*. PerkinElmer instruments, 2001.
- [11] G. Hughes, “Information on the mcplib02 photon library,” tech. rep., Los Alamos National Laboratory report LA-UR-08-539 (January 23, 1993), 1993.
- [12] G.-S. Q. Q.-Y. Q. Z.-Y. C. Tsing-Lien Changa, Wen-Jun Lib, “Absolute isotopic composition and atomic weight of germanium,” *International Journal of Mass Spectrometry*, vol. 189, pp. 205 – 211, 1999.
- [13] “Standard test procedure for germanium gamma-ray detectors,” *IEEE Std 325-1996*, 1997.

# Popularized summary in Swedish

*Mattias Jönsson*

## På jakt efter radionuklider

Efter en kärnkraftsolycka kan stora mängder radioaktivitet spridas i naturen. För att kartlägga radioaktiviteten krävs noggranna mätningar. Ett problem som kan uppstå är att det strålar så kraftigt att känsliga instrument inte hinner med. De första veckorna efter Tjernobylyckan 1986 skulle dagens känsliga halvledardetektorer haft svårt att mäta på flera ställen även i Sverige, t.ex. i Gävletrakten där det radioaktiva nedfallet var som kraftigast. I Ukraina hade det varit omöjligt. En kollimator som skärmar detektorn har visat sig vara en möjlig lösning på problemet.

Radionuklider är instabila atomer som emitterar gammafotoner då de sönderfaller. Gammafotoner är elektromagnetisk strålning med hög energi. Genom att mäta gammafotonernas energi med en gammaspektrometer kan man identifiera vilken radionuklid som sönderfallit. Olika radionuklider har olika egenskaper som t.ex. påverkar hur de sprids i naturen. Det viktigt att snabbt kunna kartlägga och identifiera de radionuklider som spridits efter en kärnkraftsolycka för att minimera de ekonomiska och medicinska konsekvenserna av strålningen.

En gammaspektrometer kan bara mäta en foton åt gången. Varje gång en foton träffar detektorn tar det ett antal mikrosekunder att analysera fotonens energi och spara informationen. Under tiden då en foton blir registrerad kommer systemet vara paralyserat och missa nya fotoner. Datorn som styr mätningen försöker korrigera mätvärdet för förlusten av mättid men detta inför alltid en osäkerhet i mätningen.

En lösning på problemet kan vara att göra elektroniken i detektorn snabbare, men tyvärr medför det att man minskar detektorns precision. För att identifiera en radionuklid krävs det att gammafotonens energi kan mätas med god precision. En annan lösning, den som vi valt att tillämpa, är att skärma detektorn från strålningen så att färre fotoner träffar detektorn. Skärmningen sker med en så kallad kollimator. Konstruktionen reducerar kraftigt fotonflödet i detektorn och gör det möjligt att mäta med god precision i betydligt kraftigare strålfält än tidigare. Kollimatoren som vi har tillverkat har en öppning som roteras runt detektorn. Då öppningen riktas mot en strålkälla kommer detektorn registrera fler fotoner. Genom att rotera kollimatoren kan detektorn användas som en radar som skannar av omgivningen för att hitta en liten strålkälla eller kartlägga en radioaktiv beläggning på marken.



Handledare: **Christer Samuelsson, Karl Östlund**

Examensarbete 30 hp i medicinsk strålningsfysik vt 2010

Avdelningen för medicinsk strålningsfysik, Institutionen för kliniska vetenskaper, Lunds universitet.

I samarbete med Strålsäkerhetsmyndigheten